1989

User-Friendly Model for the Energy Distribution of Electrons from Proton or Electron Collisions

M. Eugene Rudd
University of Nebraska - Lincoln, erudd@unl.edu

Published in *Nuclear Tracks and Radiation Measurements,* Vol. 16, No. 2/3, pp. 213-218, 1989. (Formerly *International Journal of Radiation Instrumentation, Part D*)

Submitted October 20, 1988.

User-Friendly Model for the Energy Distribution of Electrons from Proton or Electron Collisions

M. Eugene Rudd

Department of Physics and Astronomy, University of Nebraska–Lincoln, Lincoln, NE 68588-0111, U.S.A.

Abstract:
A model is presented which gives cross sections (differential in the ejected secondary electron energy) for the ionization of atoms and molecules in proton or electron collisions. The model is in the form of an analytical equation which holds for all primary and secondary energies and for any target gas for which certain parameters are known. The accuracy is estimated to be 15-20%. The model is based on the classical binary encounter model modified to agree with the Bethe theory at high energies and, for proton impact, with the molecular promotion model at low energies. For multi-shell targets, the partial cross sections for the shells, are added. The model equation may be integrated to yield such quantities as the total ionization cross section, the stopping cross section due to ionization, and the average secondary electron energy. For proton impact the integrations must be done numerically or by using approximations. For electron impact the equation is simpler and may easily be analytically integrated.

1. Introduction

In any study involving the deposition of energy by energetic charged particles traversing matter, the ejection of secondary electrons in collisions with individual atoms is of central interest, since it is the elementary process involving the greatest energy transfer. For large energy ranges it is also the most likely process. Besides a knowledge of the total cross sections for this process as a function of energy for a variety of targets, the user often needs to know the angular and energy distribution of the ejected electrons. Cross sections that are differential in the angle and secondary energy have been measured for proton impact starting in the early 1960s and for electron impact beginning in the early 1970s. While such doubly differential cross sections (DDCS) measured at different laboratories show a generally good agreement, there are ranges of parameters for which there are large discrepancies. It is especially difficult to make accurate measurements at low primary energies (below about 30 keV for protons, or 100 eV for electrons) and at low secondary energies (below about 15 eV).

Because of these discrepancies, a potential user is faced with the task of choosing among several experimental results. A further problem is that the measurements may not have been made at the required energies or for the targets needed.

Ab initio calculations of these DDCS or the singly differential cross sections (SDCS) obtained by integration over angle have been made by a number of methods. These include the classical binary encounter approximation (BEA) methods (Williams, 1927; Thomas, 1927; Gryzinski, 1965; Vriens, 1967), the Born approximation (Kuyatt and Jorgensen, 1963; Madison, 1973; Rudd and Madison, 1976), and Monte Carlo methods (Bonsen and Banks, 1971; Olson and Salop, 1977; McKenzie and Olson, 1987). Not only is the accuracy of these methods limited, but they are also useful only at high impact energies, i.e. energies for which the projectile velocity is much greater than the orbital electron velocity. In addition, the Born approximation requires a knowledge of initial- and final-state wave functions, and this information is not generally available, except for the simplest targets.

Miller and co-workers (1983,1987), and Inokuti *et al.* (1987) have developed semi-empirical models for the SDCS but these, too, are useful only at high energies.

In the present model for proton collisions, SDCS are given by a simple analytic equation containing three adjustable parameters. One of these is a dimensionless parameter near unity which is independent of proton energy but is slightly different for different targets. The other two parameters are functions of the primary energy which have been fitted by equations with four and five target parameters, respectively. The equation for electron impact is somewhat simpler, containing only two adjustable parameters. The functions describing these two parameters require a total of only four target parameters.

The SDCS equations are based on the BEA equation given by Williams (1927). They have been modified in such a way that they agree with Bethe's well-known treatment of the Born approximation (see Inokuti, 1971) at high en-

ergies, and they give the correct dependence above the kinematic cutoff. For protons of low primary energies they have been further modified to agree with the molecular promotion model (Rudd, 1979). A preliminary version of this model was given by Rudd (1987) and later presented in more detail (Rudd, 1988). The emphasis in the present paper is on the use of the model rather than its derivation (which may be found in the other papers).

2. The Model For Proton Impact

The quantities of interest in specifying the SDCS are the incident proton energy E_p, the ejected secondary energy W, and the number N of electrons in the target atom or molecule with binding energy I. It is convenient to define the electron velocity-equivalent energy as $T = E_p/\lambda$ where λ is the ratio of the proton to the electron mass. The model equation is most conveniently expressed in terms of two dimensionless quantities, the reduced secondary energy $w = W/I$ and the reduced projectile velocity $v = (T/I)^{1/2}$. The SDCS is then

$$\sigma(w) = \frac{S}{I}\,\frac{F_1 + F_2 w}{(1+w)^3\,[1 + e^{\alpha(w - w_c)/v}]} \qquad (1)$$

$S = 4\pi a_0^2 N(R/I)^2$, where a_0 is the Bohr radius and R is the rydberg of energy (13.6 eV). The quantity w_c is the kinematic cutoff energy where the cross section begins to fall off exponentially. This is given by $w_c = 4v^2 - 2v - R/4I$. F_1, F_2, and α are the three adjustable fitting parameters for an electron spectrum at a given proton energy. Figure 1 shows the fit of the model to experimental data for protons on hydrogen at three widely separated energies. Although the shape changes with energy, the model equation fits well at all energies.

Using all known SDCS data for each target, values of F_1, F_2, and α were determined by fitting the equation to the energy spectra. The parameter α was found to be nearly independent of proton energy. The other two parameters varied with E_p in a fairly consistent way as shown in the example in Figure 2 for water vapor. It was found possible to fit the energy variation of these two parameters with equations which also yielded total cross sections in agreement with the recommended values of Rudd et al. (1985). The equations for F_1 and F_2, are each combinations of low and high energy asymptotic forms:

$$F_1 = L_1 + H_1$$

and

$$F_2 = L_2 H_2/(L_2 + H_2),$$

where

$$H_1 = A_1 \ln(1 + v^2)/(v^2 + B_1/v^2),$$

$$H_2 = A_2/v^2 + B_2/v^4,$$

$$L_1 = C_1 v^{D_1}/(1 + E_1 v^{(D_1 + 4)})$$

and

$$L_2 = C_2 v^{D_2}. \qquad (2)$$

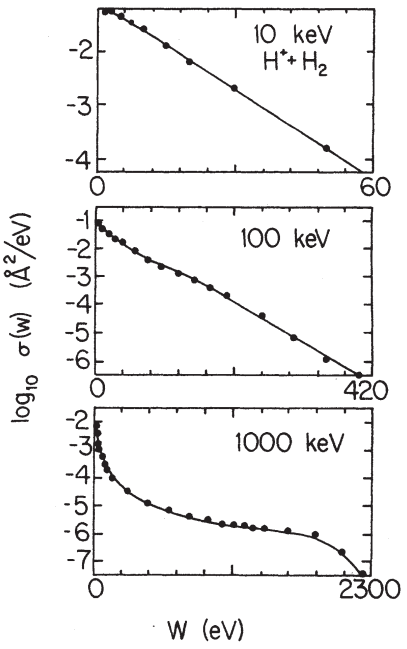

Figure 1. Energy distributions of secondary electrons from proton collisions with hydrogen molecules. The 10 and 100 keV data are from Rudd (1979), and the 1000 keV data are from Toburen and Wilson (1972). The lines are the fits of the model.

The ten target parameters $A_1 \ldots E_1$, $A_2 \ldots D_2$, and α, completely specify the cross sections at all combinations of primary proton and secondary electron energies. Tables of values of these parameters for five target gases are given in Table 1. Table 2 contains the binding energies for these targets, derived from data given by Lotz (1968) and Siegbahn et al. (1969). Figure 3 shows the values of F_1 and F_2 calculated from Equation (2) for four different targets.

3. Multi-Shell Targets

In this model, targets with more than one shell are treated by calculating separately the cross section contributions from each shell and then adding them together. Usually the outermost shell contributes most of the cross section while the deep inner shells contribute little. However,

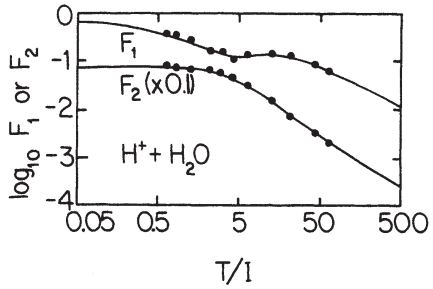

Figure 2. Values of the fitting parameters F_1 and F_2 as a function of the impact energy for $H^+ + H_2O$ collisions. The points are from fitting experimental data of Bolorizadeh and Rudd (1986), and Toburen and Wilson (1977).

Table 1. Target parameters

	H_2	He	Kr	H_2O	N_2	Inner shells
A_1	0.96	1.02	1.44	0.97	1.05	1.25
B_1	2.6	2.4	7.0	8.2	6.8	0.5
C_1	0.38	0.7	0.3	0.4	0.7	2.0
D_1	0.23	1.15	–0.8	–0.3	–0.3	2.0
E_1	2.2	0.7	0.5	0.38	1.15	3.0
A_2	1.04	0.84	1.57	1.04	1.0	1.1
B_2	5.9	6.0	5.0	17.3	5.9	1.3
C_2	1.15	0.7	1.49	0.76	0.87	1.0
D_2	0.2	0.05	–1.0	0.04	–0.6	0.3
α	0.87	0.87	0.77	0.64	0.71	0.62

the cutoff energy depends on the binding energy and is therefore different for different shells. At intermediate primary energies and at secondary energies above the cutoff for the outermost shell, the inner shell contributions may dominate. This is shown in Figure 4 for krypton where the 3*d* and 3*p* shells are dominant at high energies. The fit for water vapor at three energies is shown in Figure 5. In both Figures 4 and 5 the quantity log *Y* is plotted on the *y*-axis. *Y* is defined as the ratio of the measured or calculated cross section by the Rutherford cross section, the latter being given by $\sigma_R = 4\pi a_0^2 R^2 / T(W + I)$. Plotting *Y* instead of the cross section is a well known procedure which reduces the large range of values on the *y*-axis.

Strictly speaking, a different set of target parameters is needed for each shell, but with the data presently available it was not possible to determine so many parameters. However, since the inner shells contribute relatively little in most cases, the following procedure was used. The target electrons were divided into two categories, the outer or near-outer shells and the deep inner shells. Arbitrarily, these were chosen on the basis of whether the binding energies are less than or greater than twice that of the outermost shell. The target parameters for the first group were all taken to be the same as for the outermost shell and were

Table 2. Binding energies

	N	*I*(eV)
H_2 1*s*	2	15.4
He 1*s*	2	24.6
Kr 4*p*	4	14.0
Kr 4*p*	2	14.7
Kr 4*s*	2	27.5
Kr 3*d*	10	94.3
Kr 3*p*	6	217
H_2O $1b_1$	2	12.6
H_2O $2a_1$	2	14.7
H_2O $1b_2$	2	18.4
H_2O $1a_1$	2	32.2
H_2O 01*s*	2	540
N_2 $\sigma_g 2p$	2	15.6
N_2 $\pi_u 2p$	2	16.9
N_2 $\sigma_u 2s$	2	18.7
N_2 $\sigma_g 2s$	2	37.3
N_2 *N*1*s*	4	410

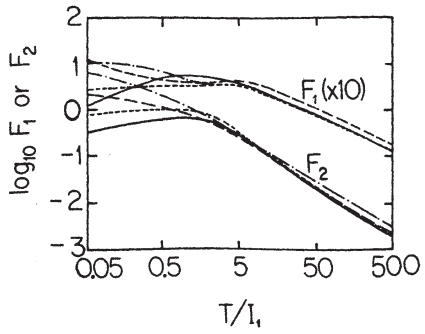

Figure 3. Values of the parameters F_1 and F_2 for four targets as functions of the impact energy. The solid line shows helium, the long dashed line, nitrogen, the short dashed line, hydrogen, and the dash-dot line, krypton.

determined by fitting to the experimental data as described above. The inner shells were assumed to have a different set of parameters which were the same for all inner shells of all targets. Only approximate values of this set could be determined, but in most cases this was sufficient since they usually make only a small contribution. The suggested set of inner-shell parameters is also given in Table 1.

4. Integration of the Model Cross Sections

Since an analytical expression is available for the SDCS, it is a simple matter to calculate a number of related quantities which are useful in a variety of applications.

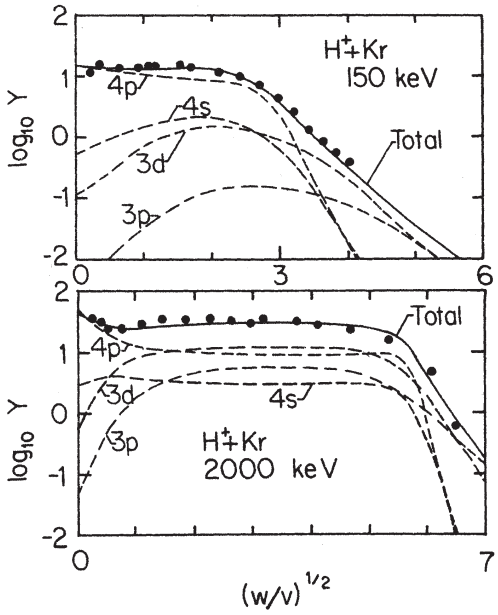

Figure 4. Energy distributions of electrons from H^+ + Kr collisions. The points are from experimental data; at 150 keV from Cheng and Rudd (1988), and at 2000 keV from Manson and Toburen (1977). The dashed lines are contributions due to individual shells, and the solid lines are totals. *Y* is the ratio of the cross section to the Rutherford cross section (see text).

The total cross section for the ejection of electrons is given by

$$\sigma_- = I \int_0^\infty \sigma(w)\, dw. \quad (3)$$

This integration is useful for normalizing the SDCS because the total cross sections are known relatively well. All available experimental measurements of σ_- for proton impact were reviewed (Rudd et al., 1985), and recommended values for many targets were given. The stopping cross section due to ionization is given by

$$\sigma_{st} = (I^2/R) \int_0^\infty (w+1)\, \sigma(w)\, dw. \quad (4)$$

The average ejected electron energy is calculated from

$$W_{av} = (I^2/\sigma_-) \int_0^\infty w\sigma(w)\, dw. \quad (5)$$

Electrons ejected with energies greater than the ionization potential (i.e. $W > I$) are able to cause further ionization. The fraction of electrons with $W > I$ is obtained from

$$f_I = (I/\sigma_-) \int_0^\infty \sigma(w)\, dw. \quad (6)$$

It is equally easy to obtain the fraction of secondaries with energies greater than any other given energy.

These integrations may be performed for proton impact either by numerical methods or analytically (with approximations). Rudd (1988) gives an approximate equation for σ_- which is very accurate at high energies, fairly good at low energies, and has about a 25% error at an intermediate energy. A similar approximate equation is given for σ_{st}.

Values of σ_{st} for three targets are given in Figure 6, along with measured values of stopping cross sections. Ionization is expected (Wilson, 1972) to contribute 78–85% of the total stopping cross section for hydrogen above 300 keV. As seen in the figure, this model gives values which are 80-85% of the total for H_2 and 80-86% for He, in excellent agreement with expectations. In the case of water vapor, however, the model yields some values in excess of the totals. Since the model is based firmly on experimental SDCS,

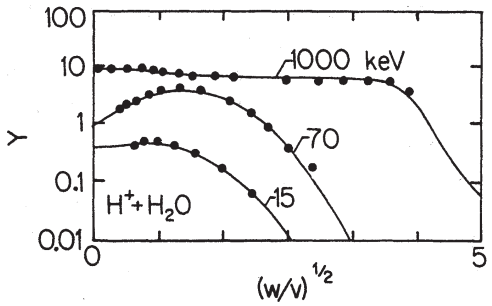

Figure 5. Energy distributions of electrons from $H^+ + H_2O$ collisions. The points, are from experimental data; at 15 and 70 keV from Bolorizadeh and Rudd (1986), and at 1000 keV from Toburen and Wilson (1977). The lines are the calculated values from the model.

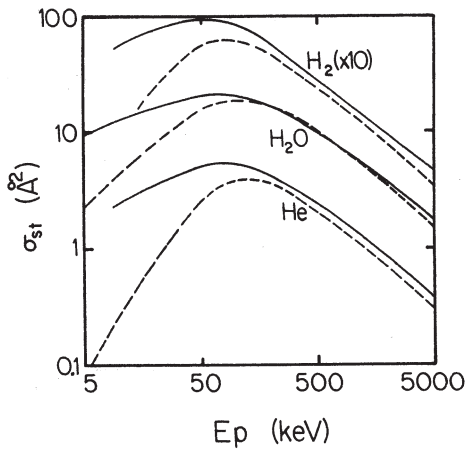

Figure 6. Stopping cross section as a function of impact energy for protons in three different gases. The dashed lines show the calculations of the contribution due to ionization using the present model, and the solid lines show the total stopping cross sections, for H_2 and He (Whaling, 1958) and for H_2O (ICRU, 1970).

this may indicate that the total stopping cross sections from the tables (ICRU, 1970) are too low.

Figure 7 shows the average energy calculated for three targets. This quantity increases with primary energy until the reduced velocity v is approximately three, after which it levels off.

It might be expected that the higher the impact energy, the larger the fraction of electrons ejected with energies greater than I. However, as seen in Figure 7, this fraction rises until $v = 2$, after which the fraction actually decreases slightly.

5. The Model for Electron Impact

The molecular promotion mechanism which gave rise to the factor containing the exponential in the proton model is not present in the case of electron impact, thus simplifying the result. The equation for electron impact is

$$\sigma(w) = (S/I)\, [F_1 + F_2(1+w)]/(1+w)^2. \quad (7)$$

An additional small change has been made, in that F_2 is multiplied by $(1 + w)$ instead of by w as in the proton case. The primary energy dependences of F_1 and F_2 are also simpler. In terms of the reduced primary energy $t = T/I$, they may be expressed as

$$F_1 = A_1 (1 - e^{-B_1 t}) \ln(t)/t \quad (8)$$

and

$$F_2 = A_2/(t + B_2). \quad (9)$$

In these equations only four target parameters, A_1, B_1, A_2, and B_2, are needed. As in the proton case, A_1 is closely related to the optical oscillator strength, and in order for the expressions for the total cross section and the stopping cross section to agree with the corresponding Bethe expressions at high energies, we must have $A_1 + A_2 = 2$.

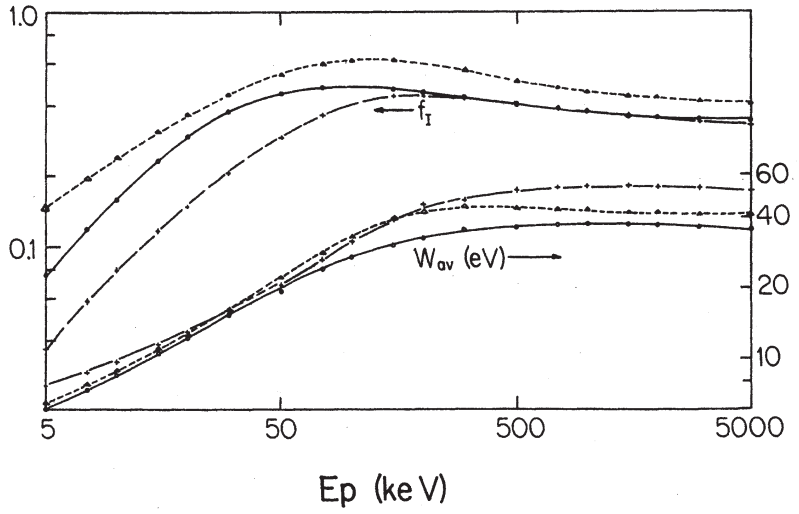

Figure 7. Values, calculated from the model, of the average secondary energy W_{av} and of the fraction f_I of secondary electrons with energies greater than the first ionization potential of the target for proton impact. The solid line shows hydrogen, the long dashed line, helium and the short dashed line, water vapor.

Figure 8 shows experimental data for helium by several investigators plotted as Y, the ratio of the cross section to the Rutherford cross section. Also shown are the calculations from the model for $A_1 = 0.94$, $B_1 = 0.28$, $A_2 = 0.70$, and $B_2 = 4.3$.

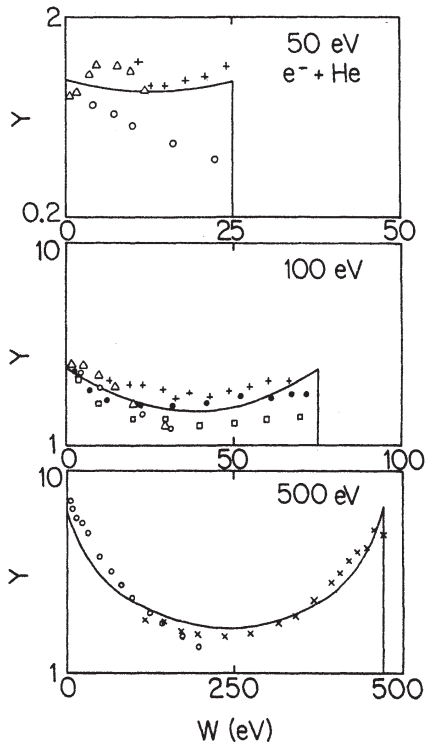

Figure 8. Energy spectra of secondary electrons from e^- + He collisions at three energies. The lines are calculations from the present model. Experimental data: + (Crooks, 1972); Δ (Shyn and Sharp, 1979); ● (Goodrich, 1937); □ (Rudd and DuBois, 1977); ○ (Opal *et al.*, 1972); × (Oda, 1975). Goodrich's data have been multiplied by 1.5.

Equation (7) is easily integrated without approximations. In the case of electrons, the upper limit of W is $T - I$ which makes $t - 1$ the upper limit of w. Some of the results are

$$\sigma_- = I \int_0^{t-1} \sigma(w)\, \mathrm{d}w = S(t-1)[F_1(t+1) + 2tF_2]/2t^2 \tag{10}$$

$$\sigma_{st} = (I/\mathrm{R}) \int_0^{t-1} (w+1)\, \sigma(w)\, \mathrm{d}w = (SI/\mathrm{R})[F_1(1 - 1/t) + F_2 \ln(t)] \tag{11}$$

6. Conclusions

A simple analytical equation has been presented which yields the energy distribution of secondary electrons from collisions with incident protons or electrons. At any given primary energy, three adjustable parameters are needed for proton impact, and two for electron impact. The primary energy dependence of these parameters is further described by equations with nine target parameters for protons and four for electrons. Values of these parameters for several targets are given, which allow easy computation of cross sections for any combination of primary and secondary energies.

By numerical or analytical integration of the model equations, one may calculate total ionization cross sections, stopping cross sections due to ionization, average secondary electron energy, and the fraction of electrons ejected with energies above any given value.

These models should be useful in situations involving the transfer of energy by fast charged particles during collisions with atoms or molecules.

References

Bolorizadeh M. A. and Rudd M. E. (1986) Angular and energy dependence of cross sections for ejection of electrons from water vapor. II. 15-150 keV proton impact. *Phys. Rev.* **A33**, 888–892.

Bonsen T. F. M. and Banks D. (1971) Angular distribution of electrons ejected by charged particles. III. Classical treatment of forward ejection. *J. Phys. B. Atom. Molec. Phys.* **4**, 706–714.

Cheng Wen-qin and Rudd M. E. (1988) Differential cross sections for ejection of electrons from rare gases by 7.5–150 keV protons. *Phys. Rev.* **A39**, 2359–2366.

Crooks G. B. (1972) Energy and angular distributions of scattered and ejected electrons produced by 50-800 eV electrons in helium. Ph. D. dissertation, University of Nebraska, Lincoln, Nebraska, U.S.A.

Goodrich M. (1937) Electron scattering in helium. *Phys. Rev.* **52**, 259-266.

Gryzinski M. (1965) Two-particle collisions. II. Coulomb collisions in the laboratory of coordinates. *Phys. Rev.* **138**, A322-A335.

ICRU (1970) Linear energy transport. ICRU Report No. 16, p. 32, International Commission on Radiation Units and Measurements, Washington, DC, U.S.A.

Inokuti M. (1971) Inelastic collisions of fast charged particles with atoms and molecules—the Bethe theory revisited. *Rev. Mod. Phys.* **43**, 297-347.

Inokuti M., Dillon M. A., Miller J. H., and Omidvar K. (1987) Analytic representation of secondary-electron spectra. *J. Chem. Phys.* **87**, 6967-6972.

Kuyatt C. E. and Jorgensen T. Jr (1963) Energy and angular dependence of the differential cross section for production of electrons by 50-100 keV protons in hydrogen gas. *Phys. Rev.* **130**, 1444-1455.

Lotz W. (1968) Subshell binding energies of atoms and ions from hydrogen to zinc. *J. Opt. Soc. Am.* 7, 915-921.

Madison D. H. (1973) Angular distributions of electrons ejected from helium by proton impact. *Phys. Rev.* **A8**, 2449–2455.

Manson S. T. and Toburen L. H. (1977) Energy and angular distribution of electrons ejected from Kr by 1 MeV proton impact ionization: Theory and experiment. In *10th Int. Conf. Physics Electron. Atom. Collisions,* abstracts of papers, p. 99. Commissariat à l'Energie Atomique, Paris.

McKenzie, M. L. and Olson R. E. (1987) Ionization and charge exchange in multiply-charged ion-helium collisions at intermediate energies. *Phys. Rev.* **A35**, 2863–2868.

Miller J. H., Toburen L. H., and Manson S. T. (1983) Differential cross sections for ionization of helium, neon, and argon by high-velocity ions. *Phys. Rev.* **A27**, 1337–1344.

Miller J. H., Wilson W. E., Manson S. T. and Rudd M. E. (1987) Differential cross sections for ionization of water vapor by high-velocity bare ions and electrons. *J. Chem. Phys.* **86**, 157–162.

Oda Nobuo (1975) Energy and angular distributions of electrons from atoms and molecules by electron impact. *Radiat. Res.* **64**, 80–95.

Olson R. E. and Salop A. (1977) Charge-transfer and impact-ionization cross sections for fully and partially stripped positive ions colliding with atomic hydrogen. *Phys. Rev.* **A16**, 531–541.

Opal C. B., Beaty E. C. and Peterson W. K. (1972) Tables of secondary-electron-production cross sections. *Atom. Data* **4**, 209–253.

Rudd M. E. (1979) Energy and angular distributions of secondary electrons from 5-100 keV proton collisions with hydrogen and nitrogen molecules. *Phys. Rev.* **A20**, 787–796.

Rudd M. E. (1987) Singly differential cross sections for producing secondary electrons from hydrogen gas by keV to MeV proton collisions. *Radiat. Res.* **109**, 1–11.

Rudd M. E. (1988) Differential cross sections for secondary electron production by proton impact. *Phys. Rev.* **A38**, 6129–6137.

Rudd M. E. and Madison D. H. (1976) Comparison of experimental and theoretical electron ejection cross sections in helium by proton impact from 5 to 100 keV. *Phys. Rev.* **A14**, 128–136.

Rudd M. E. and DuBois R. D. (1977) Absolute doubly differential cross sections for ejection of secondary electrons from gases by electron impact. I. 100-200 eV electrons on helium. *Phys. Rev.* **A16**, 26–32.

Rudd M. E., Kim Y.-K., Madison D. H., and Gallagher J. W. (1985) Electron production in proton collisions: Total cross sections. *Rev. Mod. Phys.* **57**, 965–994.

Shyn T. W. and Sharp W. E. (1979) Doubly differential cross sections of secondary electrons ejected from gases by electron impact: 50-300 eV on helium. *Phys. Rev.* **A19**, 557–567.

Siegbahn K., Nordling C., Johansson G., Hedman J., Heden P. F., Hamrin K., Gelius U., Bergmark T., Werme L. O., Manne R., and Baer Y. (1969) *ESCA Applied to Free Molecules,* North-Holland, Amsterdam.

Thomas L. H. (1927) The effect of the orbital velocity of the electrons in heavy atoms and their stopping of alpha- particles. *Proc. Camb. Phil. Soc.* **23**, 713–716.

Toburen K. H. and Wilson W. E. (1972) Distributions in energy and angle of electrons ejected from molecular hydrogen by 0.3-1.5 MeV protons. *Phys. Rev.* **A5**, 247–256.

Toburen L. H. and Wilson W. E. (1977) Energy and angular distributions of electrons ejected from water vapor by 0.3-1.5 MeV protons. *J. Chem. Phys.* **66**, 5202–5213.

Vriens K. (1967) Binary-encounter proton-atom collision theory. *Proc. Phys. Soc.* **90**, 935–944.

Whaling W. (1958) The energy loss of charged particles in matter. In *Handbuch der Physik* (Edited by Flugge S.), Vol. XXIV, pp. 193–217. Springer, Berlin.

Williams E. J. (1927) The passage of alpha-rays and beta-rays through matter. *Nature* **119**, 489–490.

Wilson W. E. (1972) Stopping power partition and mean energy loss for energetic protons in hydrogen. *Radiat. Res.* **49**, 36-50.